

Squeezed light from conventionally pumped lasers with nonuniform spatial structure

C. M. Savage and T. C. Ralph

Department of Physics and Theoretical Physics, Australian National University, Australian Capital Territory 2601, Australia

(Received 6 April 1992)

Spatial variations of the laser mode and pumping rate are incorporated into the theory of conventionally pumped lasers that produce squeezed light. Both a quantum-mechanical theory and a heuristic statistical model are used. While variations in the laser mode are found to have a negligible effect on squeezing, variations in the pumping rate are significant. The maximum attainable squeezing is always reduced compared with the spatially uniform case. However, resonantly enhancing a low-power pump in a Fabry-Pérot cavity, rather than a ring cavity, may give better squeezing.

PACS number(s): 42.50.Dv, 42.55.-f

I. INTRODUCTION

The theory of amplitude-squeezed light generation by conventionally pumped lasers is well studied [1-7]. A simple criterion for laser squeezing is provided by an heuristic statistical model of the transitions in the lasing atoms: the pumping rate should approximately equal a spontaneous decay rate [3-5]. This condition appears to be achievable in practice [7].

In this paper the effect of nonuniform spatial structure on the squeezing is analyzed. Previous work has assumed that both the pumping rate and laser mode are constant in space; however, real lasers will generally have both transverse and longitudinal spatial structure. Since the matching of the pumping rate to a decay rate is crucial for squeezing, spatial variations in the pumping rate are potentially important.

We first analyze the effects of spatial structure on a three-level incoherently pumped laser. Both the linearized P -function theory [8,9] and the statistical model are used. The latter agrees well with the P -function theory, but can only accommodate spatial variations in the pumping rate. The statistical approach allows a relatively simple analysis which we also apply to the four-level coherently pumped laser.

Our conclusion is that spatial variations do not greatly alter the squeezing from that predicted by spatially uniform models. Nevertheless, spatial variations in the pumping rate may be important for the quantitative comparison of theory with experiment. A potentially useful result concerns the best scheme for resonant enhancement of an optical pump. At low pumping rates the spatial oscillations of the intensity in a Fabry-Pérot cavity produce better squeezing than the longitudinally uniform field of a ring cavity.

Section II describes how spatial variations can be included in the quantum-mechanical P -function theory of a three-level incoherently pumped laser. Section III introduces the statistical model and adapts it to spatial variations in the pumping rate. In Sec. IV the preceding theory is applied to specific examples of spatially varying laser modes and pumping rates. The statistical method is used to analyze the effect of spatial variations of the

pumping field on a four-level coherently pumped laser. Section V summarizes our results.

II. QUANTUM-MECHANICAL P -FUNCTION TREATMENT

In this section we extend the usual P -function theory to include spatial variations of the laser mode and pumping rate. To keep the emphasis on the effect of spatial variation the theory is kept as simple as possible while retaining the laser squeezing.

The level scheme of our laser atoms is shown in Fig. 1. Only the essential spontaneous decay is considered. The atoms are incoherently pumped at the rate P and lasing occurs between the upper two levels $|2\rangle$ and $|3\rangle$. The spontaneous decay from the lower lasing level $|2\rangle$ occurs at the rate γ .

The laser consists of N of these atoms, grouped into M groups of N_j atoms so that spatial variations may be analyzed. Each group occupies a volume element of space over which the laser field and pumping rate are assumed to be constant. The master equation for the reduced density operator $\hat{\rho}$ for this system may be derived by standard system-reservoir techniques [10-12], and is given in Ref. [2] for the case of no spatial variations. With spatial variations it generalizes to [8,9].

$$\frac{\partial}{\partial t} \hat{\rho} = \frac{1}{i\hbar} [\hat{H}_{JC}, \hat{\rho}] + \frac{1}{2} (L_{\text{pump}} + \gamma L_{12}) \hat{\rho} + \kappa (2\hat{a} \hat{\rho} \hat{a}^\dagger - \hat{a}^\dagger \hat{a} \hat{\rho} - \hat{\rho} \hat{a}^\dagger \hat{a}),$$

$$L_{\text{pump}} \hat{\rho} = \sum_{j=1}^M P_j (2\hat{J}_{13j}^+ \hat{\rho} \hat{J}_{13j}^- - \hat{J}_{13j}^- \hat{J}_{13j}^+ \hat{\rho} - \hat{\rho} \hat{J}_{13j}^- \hat{J}_{13j}^+), \quad (1)$$

$$L_{12} \hat{\rho} = \sum_{j=1}^M (2\hat{J}_{12j}^- \hat{\rho} \hat{J}_{12j}^+ - \hat{J}_{12j}^+ \hat{J}_{12j}^- \hat{\rho} - \hat{\rho} \hat{J}_{12j}^+ \hat{J}_{12j}^-).$$

The \hat{J}_{mnj}^\pm are collective atomic operators for the j th group of atoms

$$\hat{J}_{nmj}^\pm = \sum_{i=1}^{N_j} \exp[\pm i\eta(\mathbf{r}_{ij})] \hat{\sigma}_{nmij}^\pm. \quad (2)$$

The σ_{nmij}^\pm are the raising and lowering operators be-

tween levels $|n\rangle$ and $|m\rangle$ for the i th atom in the j th group, and the $\eta(\mathbf{r}_{ij})$ are the mode phase factors at the position \mathbf{r}_{ij} of the atom. κ is the cavity amplitude decay rate. \hat{H}_{JC} is the Jaynes-Cummings Hamiltonian for the interaction between the atoms and the laser cavity mode, which has boson annihilation and creation operators \hat{a} and \hat{a}^\dagger ,

$$\hat{H}_{JC} = i\hbar \sum_{i=1}^{N_j} g_j (\hat{a}^\dagger \hat{J}_{23j}^- - \hat{a} \hat{J}_{23j}^+) . \quad (3)$$

g_j is the Jaynes-Cummings coupling strength for the j th group of atoms given by

$$g_j = \left[\frac{3\pi\gamma_L c^3}{2\omega^2} \right]^{1/2} |u(\mathbf{r}_{ij})| = g_0 |u(\mathbf{r}_{ij})| , \quad (4)$$

where ω is the angular frequency of the laser transition, γ_L its free-space spontaneous-emission rate, and $u(\mathbf{r}_{ij})$ is the normalized mode function for the laser mode. Particular mode functions are discussed in Sec. IV. In the limit of large numbers of atoms N_j in each group a Fokker-Planck equation for the positive- P quasiprobability distribution function [12,13] can be derived. To this correspond the stochastic differential equations [12,14]

$$\begin{aligned} \dot{\alpha} &= -\kappa\alpha + \sum_{j=1}^M g_j J_{23j}^- , & \dot{\alpha}^\dagger &= -\kappa\alpha^\dagger + \sum_{j=1}^M g_j J_{23j}^+ , \\ \dot{J}_{23j}^- &= -\frac{\gamma}{2} J_{23j}^- + g_j \alpha J_{Dj} + \Gamma_{23-j} , \\ \dot{J}_{23j}^+ &= -\frac{\gamma}{2} J_{23j}^+ + g_j \alpha^\dagger J_{Dj} + \Gamma_{23+j} , \\ \dot{J}_{3j} &= P_j J_{1j} - g_j (\alpha J_{23j}^+ + \alpha^\dagger J_{23j}^-) + \Gamma_{3j} , \\ \dot{J}_{Dj} &= \gamma J_{2j} + P_j J_{1j} - 2g_j (\alpha J_{23j}^+ + \alpha^\dagger J_{23j}^-) + \Gamma_{Dj} . \end{aligned} \quad (5)$$

The c -number stochastic variables introduced here correspond to the field mode and collective atomic operators previously introduced. J_{1j} , J_{2j} , J_{3j} , and J_{Dj} correspond to the collective atomic populations in the j th atomic group for levels $|1\rangle$, $|2\rangle$, and $|3\rangle$, respectively, while $J_{Dj} = J_{3j} - J_{2j}$ corresponds to the inversion on the lasing levels $|3\rangle$ and $|2\rangle$. P_j is the incoherent laser pumping rate of the j th atomic group. The Γ_j are Gaussian white noises with zero mean and whose nonzero correlations are

$$\begin{aligned} \langle \Gamma_{23-j}(t) \Gamma_{23-j}(t') \rangle &= 2g_j \alpha^\dagger J_{23j}^- \delta(t-t') , \\ \langle \Gamma_{23+j}(t) \Gamma_{23+j}(t') \rangle &= 2g_j \alpha J_{23j}^+ \delta(t-t') , \\ \langle \Gamma_{23-j}(t) \Gamma_{23+j}(t') \rangle &= (P_j J_{1j} + \gamma J_{3j}) \delta(t-t') , \\ \langle \Gamma_{23-j}(t) \Gamma_{Dj}(t') \rangle &= -\gamma J_{23j}^- \delta(t-t') , \\ \langle \Gamma_{23+j}(t) \Gamma_{Dj}(t') \rangle &= -\gamma J_{23j}^+ \delta(t-t') , \\ \langle \Gamma_{Dj}(t) \Gamma_{3j}(t') \rangle &= -g_j (\alpha J_{23j}^+ + \alpha^\dagger J_{23j}^-) \delta(t-t') , \\ \langle \Gamma_{Dj}(t) \Gamma_{Dj}(t') \rangle &= -2g_j (\alpha J_{23j}^+ + \alpha^\dagger J_{23j}^-) \delta(t-t') . \end{aligned} \quad (6)$$

The stochastic differential equations for the polarizations J_{12j}^\pm and J_{13j}^\pm are ignored because they decouple from Eqs. (5), which alone determine the properties of the field.

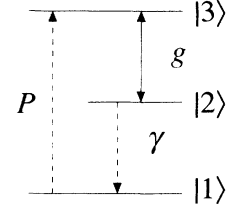


FIG. 1. Schematic diagram of the three-level incoherently pumped laser's level scheme.

The stochastic differential Eqs. (5) are solved by assuming small quantum-mechanical fluctuations about a stable steady state. The steady state is found by putting the derivatives on the left-hand side of Eqs. (5) equal to zero, dropping the noise terms, and solving. Equations (5) may then be linearized about the steady state. Since the phase of the laser field may be chosen arbitrarily all steady-state variables may be taken to be real. Solving the resulting coupled nonlinear algebraic equations gives [N.B. In order to maintain a manageable notation, from here on the c -number variables denote the steady-state values, instead of the stochastic variables of Eqs. (5).]

$$1 = \sum_{j=1}^M \frac{g_j^2}{\kappa} N_j \frac{\gamma/2}{(2 + \gamma/P_j)(g_j \alpha)^2 + \gamma^2/4} . \quad (7)$$

In general Eq. (7) must be solved numerically. However, for the spatially uniform case $M=1$, it has the following solution, valid provided it is positive:

$$\alpha^2 = \frac{P}{2P + \gamma} \frac{\gamma}{2g^2} \left[\frac{g^2 N}{\kappa} - \frac{\gamma}{2} \right] . \quad (8)$$

The steady-state solutions for the atomic variables are given in terms of the field by

$$\begin{aligned} J_{2j} &= N_j \left[2 + \gamma/P_j \left[1 + \frac{\gamma P_j}{4g_j^2 \alpha^2} \right] \right]^{-1} , \\ J_{Dj} &= N_j - (2 + \gamma/P_j) J_{2j} , & J_{23j}^- &= \frac{\gamma}{2g_j \alpha} J_{2j} . \end{aligned} \quad (9)$$

The stochastic differential Eqs. (5) are linearized by expressing the variables as the sum of their steady-state values and small fluctuations, denoted by a prefixed δ , and only retaining first-order terms in these small fluctuations. Following Reid [15] we also transform to Fourier space so that the equations become

$$\begin{aligned} 0 &= (-\kappa + i\omega) \delta\alpha + \sum_{j=1}^M g_j \delta J_{23j}^- , \\ 0 &= (-\kappa + i\omega) \delta\alpha^\dagger + \sum_{j=1}^M g_j \delta J_{23j}^+ , \\ 0 &= (-\gamma/2 + i\omega) \delta J_{23j}^- + g_j J_{Dj} \delta\alpha + g_j \alpha \delta J_{Dj} + \Gamma_{23-j} , \\ 0 &= (-\gamma/2 + i\omega) \delta J_{23j}^+ + g_j J_{Dj} \delta\alpha^\dagger + g_j \alpha^\dagger \delta J_{Dj} + \Gamma_{23+j} , \\ 0 &= i\omega \delta J_{3j} - P_j (\delta J_{2j} + \delta J_{3j}) - Z + \Gamma_{3j} , \\ 0 &= i\omega \delta J_{Dj} - P_j (\delta J_{2j} + \delta J_{3j}) + \gamma \delta J_{2j} - 2Z + \Gamma_{Dj} , \\ Z &\equiv g_j (J_{23j}^- \delta\alpha^\dagger + \alpha^\dagger \delta J_{23j}^- + J_{23j}^+ \delta\alpha + \alpha \delta J_{23j}^+) , \end{aligned} \quad (10)$$

The variables and noises are now functions of frequency rather than time. The noise correlations $\langle \Gamma_A(\omega)\Gamma_B(\omega') \rangle$ are given by the right-hand sides of Eqs. (6) with $\delta(t-t')$ replaced by $\delta(\omega+\omega')$. The quantity Z is introduced as a notational shorthand. Equations (10) are a system of linear algebraic equations for the small fluctuations. They can be simplified by introducing quantities corresponding to the amplitude quadrature

$$\begin{aligned} \delta X &\equiv \delta\alpha + \delta\alpha^\dagger, \quad \delta J_{X_j} = \delta J_{23j}^- + \delta J_{23j}^+, \\ \Gamma_{X_j} &= \Gamma_{23+j} + \Gamma_{23-j}. \end{aligned} \quad (11)$$

Equations (10) then become, after eliminating δJ_{1j} and δJ_{2j} ,

$$\begin{aligned} c_8 &= c_4 c_5 \left[\kappa - i\omega - \sum_{j=1}^M g_j^2 c_4 c_5 \{ J_{D_j} - c_1 c_3 2g_j \alpha J_{23j}^- [2 + c_2(\gamma - 2P_j)] \} \right]^{-1}, \\ c_7 &= c_1 c_3 c_8 2g_j \alpha, \quad c_6 = c_2 c_7 (\gamma - 2P_j), \quad c_5 = \{ 1 + c_1 c_3 c_4 2(g_j \alpha)^2 [2 + c_2(\gamma - 2P_j)] \}^{-1}, \\ c_4 &= (\gamma/2 - i\omega)^{-1}, \quad c_3 = [1 - c_1 c_2 (\gamma - 2P_j) P_j]^{-1}, \quad c_2 = (2P_j - i\omega)^{-1}, \quad c_1 = (\gamma - P_j - i\omega)^{-1}. \end{aligned} \quad (14)$$

The amplitude-squeezing spectrum of the cavity field is then

$$\begin{aligned} \langle \delta X(\omega) \delta X(-\omega) \rangle &= \sum_{j=1}^M 2g_j^2 \{ |c_8|^2 (2g_j \alpha J_{23j}^- + P_j J_{1j} + \gamma J_{3j}) \\ &\quad - 2J_{23j}^- [\gamma \operatorname{Re}(c_7^* c_8) + g_j \alpha \operatorname{Re}(c_6^* c_7) \\ &\quad + g_j \alpha |c_7|^2] \}. \end{aligned} \quad (15)$$

According to the input-output theory of Gardiner and Collett [12,16] the squeezing spectrum of the field emitted by the laser, assuming significant output coupling through one mirror only, is

$$V(\omega) = 1 + 2\kappa \langle \delta X(\omega) \delta X(-\omega) \rangle. \quad (16)$$

The predictions of this formula are considered in Sec. IV.

III. STATISTICAL MODEL

Laser squeezing is a consequence of sub-Poissonian population dynamics in the individual laser atoms [3–5]. In this section a heuristic statistical model of the pumping process is extended to the case of spatially varying pumping rates.

Since it is a Poissonian process the mean time for a spontaneous emission from one atom in the lower lasing level $|2\rangle$ is $\bar{t} = 1/\gamma$, and the variance in the emission time is $\Delta t^2 = \bar{t}^2 = (1/\gamma)^2$. However, we assume that the laser is operating under conditions such that the populations in the two lasing levels $|3\rangle$ and $|2\rangle$ are approximately equal (see Sec. IV B 1). Then electrons are only available to decay out of the lower lasing level $|2\rangle$ half the time. Consequently, the mean time for decay out of this level is

$$\begin{aligned} 0 &= (-\kappa + i\omega) \delta X + \sum_{j=1}^M g_j \delta J_{X_j}, \\ 0 &= (-\gamma/2 + i\omega) \delta J_{X_j} + g_j J_{D_j} \delta X + g_j \alpha \delta J_{D_j} + \Gamma_{X_j}, \\ 0 &= (-2P_j + i\omega) \delta J_{3j} - P_j \delta J_{D_j} - Y + \Gamma_{3j}, \\ 0 &= (P_j - \gamma + i\omega) \delta J_{D_j} + (\gamma - 2P_j) \delta J_{3j} - 2Y + \Gamma_{D_j}, \\ Y &\equiv g_j (J_{23j}^- \delta X + \alpha \delta J_{X_j}). \end{aligned} \quad (12)$$

Solving these equations for $\delta X(\omega)$ we find

$$\delta X(\omega) = \sum_{j=1}^M g_j (c_6 \Gamma_{3j} + c_7 \Gamma_{D_j} + c_8 \Gamma_{X_j}), \quad (13)$$

where the coefficients c_6 , c_7 and c_8 are given by

$\bar{t} = 2/\gamma$, and the variance is $\Delta t^2 = (2/\gamma)^2$ [5,7]. Incoherent pumping may be modeled as an inverse spontaneous decay [10], giving a pumping time mean and variance of $\bar{t} = 1/P_j$ and $\Delta t^2 = (1/P_j)^2$. Since the spontaneous emission and pumping are statistically independent processes the mean time for the combined processes is $\bar{t}_j = 1/P_j + 2/\gamma$, and the variance in the time is $\Delta t_j^2 = (1/P_j)^2 + (2/\gamma)^2$.

These atomic time statistics determine the counting statistics of the photons produced by the laser. Over a period of time T the j th atomic group produces a mean number of photons $n_j = N_j(T/\bar{t}_j)$. This relates the two stochastic variables, n_j the number of photons produced in a certain time period T , and \bar{t}_j the mean time for population to be transferred from the lower to the upper lasing level in that time period. Since the fluctuations in the mean quantities are small we can use the usual formula relating the variance in a function of a stochastic variable to the variance of the variable itself [17]

$$\left[\frac{\Delta n_j}{\bar{n}_j} \right]^2 = \left[\frac{\Delta \bar{t}_j}{\bar{t}_j} \right]^2. \quad (17)$$

This formula relates the photon statistics to the statistics of the mean time for population transfer between the laser levels. It is more useful to express the photon statistics in terms of the variance of the time for an individual transfer Δt_j^2 rather than in terms of the variance of the mean time $\Delta \bar{t}_j^2$. Since there are a mean of \bar{n}_j transitions per time period they are related by

$$\Delta \bar{t}_j^2 = \frac{\Delta t_j^2}{\bar{n}_j}. \quad (18)$$

The Fano factor is defined to be the ratio of the photon-number variance to the mean. Using Eq. (18) in Eq. (17)

we find the Fano factor for photons produced by the j th atomic group in the time T to be

$$f_j \equiv \frac{\Delta \bar{n}_j^2}{\bar{n}_j} = \frac{\Delta t_j^2}{\bar{t}_j^2}. \quad (19)$$

If T is much longer than the cavity decay time $1/(2\kappa)$, this will be the Fano factor for the photons emitted from the laser. For the three-level laser shown in Fig. 1 the Fano factor is then

$$f_j = \frac{\Delta t_j^2}{\bar{t}_j^2} = \frac{(1/P_j)^2 + (2/\gamma)^2}{(1/P_j + 2/\gamma)^2}. \quad (20)$$

If there are many spatial groups the mean photon number produced in the time T is the sum of the means for each of the groups

$$\bar{n} = \sum_{j=1}^M N_j \frac{T}{\bar{t}_j}. \quad (21)$$

Since each spatial group radiates independently of the other the total variance in the photon number is the sum of the individual variances

$$\Delta n^2 = \sum_{j=1}^M \Delta n_j^2 \quad (22)$$

and the overall Fano factor is

$$f = \frac{\Delta n^2}{\bar{n}} = \sum_{j=1}^M \left[\frac{\Delta n_j^2}{\bar{n}_j} \right] \left[\frac{\bar{n}_j}{\bar{n}} \right] = \sum_{j=1}^M f_j \frac{\bar{n}_j}{\bar{n}}. \quad (23)$$

This is the mean of the Fano factors for each spatial group weighted by the proportion of photons produced by that group. This simple formula depends only on the atomic decay rate γ and the pumping rate at each spatial group P_j .

The Fano factor of this section and the amplitude-squeezing spectral density of Sec. II are closely related. They are approximately equal provided the quantum fluctuations in the field amplitude are small compared to the steady-state field amplitude. This can be confirmed by expressing the photon number variance in terms of the Fourier-space field variables of Sec. II,

$$\begin{aligned} \delta n(\omega=0)^2 &= \Delta \{ [\alpha + \delta\alpha^\dagger(\omega=0)][\alpha + \delta\alpha(\omega=0)] \}^2 \\ &\approx \alpha^2 \langle \delta X(\omega=0) \delta X(\omega=0) \rangle \\ \implies f &= \frac{\Delta n(\omega=0)^2}{\alpha^2} \approx \langle \delta X(\omega=0) \delta X(\omega=0) \rangle, \end{aligned} \quad (24)$$

where we have noted that $\bar{n} = \alpha^2$ and Δn^2 is a zero-frequency quantity, since T is required to be the longest time scale in the problem.

IV. SPATIAL STRUCTURE

After introducing the spatial mode functions in Sec. IV A we use the preceding theory to calculate their effect on the laser squeezing in Sec. IV B. The theory is quite general, but we consider only Gaussian transverse and

sinusoidal longitudinal variations. The former describes cavity and fiber modes fairly well. The sinusoidal variation describes a pump resonantly enhanced in a Fabry-Pérot cavity. The figures have been chosen with parameters appropriate for a single mode fiber laser, since we believe this type of laser to be a candidate for displaying squeezing [7].

A. Mode functions

The mode functions occurring in the Jaynes-Cummings coupling strength, Eq. (4), are normalized so that the integral of their modulus squared over all space is one. The particular mode functions we consider in this paper are given in Table I. The Gaussian transverse mode is appropriate for either a cavity, or a fiber if truncated at the core radius. The sinusoidal longitudinal mode describes a Fabry-Pérot cavity mode. We assume pump depletion is negligible.

The mode functions of Table I will also be used to describe the spatial variation of the pumping strength

$$P_j = P_I |u(\mathbf{r}_j)|^2 L. \quad (25)$$

Although it is not essential, we now assume that the pumping is optical. The factor of L occurs because it is intensity rather than energy density that is important for pumping, so the normalization factor is the area V_N/L rather than the volume V_N . P_I is the pumping rate integrated over the mode's cross-sectional area, and averaged over a wavelength longitudinally, for longitudinally varying modes. It is proportional to the total pumping power and is hence the appropriate quantity to hold fixed when comparing the laser's behavior for different pump modes. It is related to the total pumping power by

$$P_{\text{power}} = \frac{\hbar\omega_p}{\sigma_p} P_I, \quad (26)$$

where $\hbar\omega_p$ is the energy of a pump photon and σ_p is the pump absorption cross section.

It is more convenient to calculate with the volume density of atoms ρ than with the number of atoms in a group N_j . Hence the scaled Jaynes-Cummings coupling strength \bar{g}_0 is useful,

$$\bar{g}_0 \equiv g_0 \sqrt{V_N}. \quad (27)$$

TABLE I. Spatial mode functions considered in this paper. The normalized mode function is $|u(\mathbf{r})|$. V_N is the normalization volume. The mode functions are zero outside a region of length L , and for the nontransversely varying mode functions, outside a cylinder of cross-sectional area A . r is the transverse radial coordinate and z is the longitudinal coordinate.

Name	$ u(\mathbf{r}) $	V_N
Uniform	$1/\sqrt{V_N}$	AL
Transverse Gaussian	$\exp[-(r/W)^2]/\sqrt{V_N}$	$\frac{1}{2}\pi W^2 L$
Standing wave	$\cos(kz)/\sqrt{V_N}$	$\frac{1}{2}AL$
Gaussian plus Standing wave	$\cos(kz)\exp[-(r/W)^2]/\sqrt{V_N}$	$\frac{1}{4}\pi W^2 L$

It is also convenient to calculate with scaled variables, denoted by a tilde,

$$\tilde{\alpha} = \alpha / \sqrt{\rho V_M}, \quad \tilde{J}_j = J_j / N_j. \quad (28)$$

Since V_M is the laser medium volume these variables refer to the field amplitude per root atoms, and to the polarization, and population per atom. They are advantageous for numerical calculations because the scaled field is independent of the normalization volume, as can be seen by substituting \tilde{g}_0 and $\tilde{\alpha}$ into the steady-state Eq. (7) and making the dependence of the mode function on the normalization volume explicit. If they are used in the formulas of Sec. II, g_j occurs multiplied by either $\sqrt{N_j}$ or $\sqrt{\rho}$. In terms of the scaled \tilde{g}_0 ,

$$\begin{aligned} g_j \sqrt{\rho} &= g_0 |u(\mathbf{r}_j)| \sqrt{\rho} = \tilde{g}_0 |u(\mathbf{r}_j)|, \\ g_j \sqrt{N_j} &= g_j \sqrt{\rho \Delta V_j} = \tilde{g}_0 |u(\mathbf{r}_j)| \sqrt{\Delta V_j}, \end{aligned} \quad (29)$$

where ΔV_j is the medium volume occupied by the j th atomic group.

B. The effect of spatial structure on squeezing

In this section we calculate the squeezing with nonuniform laser modes and pumping rates. The linearized P -function method is suitable for both cases while the statistical model can only model a varying pumping rate. The results show that the spatial structure of the laser mode has a negligible effect on the squeezing, while under certain conditions a spatially varying pump rate can enhance the squeezing.

1. The laser mode

A nonuniform laser mode implies the local field and the Jaynes-Cummings coupling strength are nonuniform. This will degrade the squeezing if the stimulated emission rate for certain groups becomes comparable to the other atomic rates. For then the laser transition will be slowed and become an additional noise source [7]. Fortunately such atoms will also contribute few laser photons. Since the contribution of each atomic group to the squeezing is in proportion to the number of photons it contributes, see Eq. (23), their influence on the squeezing will be proportionately small.

The combination of parameters that determines the significance of spatial variations in the laser mode is \tilde{g}_0^2/κ . In the spatially uniform case this equals $g^2 N/\kappa$. According to the expression for the spatially uniform steady-state field, Eq. (8), if it is much larger than $\gamma/2$ then the field is independent of g . The populations on the lasing levels are then also approximately equal, as discussed in Sec. II. So if the inequality

$$\tilde{g}_0^2/\kappa \gg \gamma/2 \quad (30)$$

is satisfied we anticipate that spatial variations in g_j will not affect the field strength much. We now choose some typical parameters to see if this inequality is likely to be satisfiable in practice. Using parameters typical of rare-earth ions, $\gamma_L \approx 100 \text{ s}^{-1}$ and $\omega \approx 10^{15} \text{ s}^{-1}$, in Eq. (4) gives $g_0^2 \approx 0.01 \text{ m}^3 \text{ s}^{-2}$. An ionic density of $\rho \approx 10^{26} \text{ m}^{-3}$ gives

$\tilde{g}_0^2 \approx 10^{24} \text{ s}^{-1}$. A cavity decay rate of $\kappa \approx 10^8 \text{ s}^{-1}$ gives $\tilde{g}_0^2/\kappa \approx 10^{16} \text{ s}^{-1}$. So the inequality (30) is satisfied provided the atomic decay rate is much slower than this, which is typically the case.

We have performed a numerical calculation which verifies the preceding general considerations. We used the theory of Sec. II to compare the maximum squeezing with a spatially uniform laser mode to that with a Gaussian laser mode. The Gaussian waist was chosen to be half the medium radius, $W/R=0.5$, so that at the medium's edge $r=R$ the mode function squared is a factor of e^{-8} less than at the center $r=0$. For the spatially uniform case the maximum squeezing of $V(\omega=0)=0.5$ occurs for the matched pumping rate $P=\gamma/2$. Numerical calculations show that with Gaussian structure the spectral variance remains below 0.55, $V(\omega=0) \leq 0.55$, provided $\tilde{g}_0^2/\kappa \geq 500\gamma$, which is consistent with the inequality (30). The results of this section lead us to expect that the atom-cavity coupling can be made sufficiently strong for spatial variations in the laser mode to have a negligible effect on squeezing.

2. The pumping rate: three-level laser

In this section we compare the squeezing produced by incoherently pumped three-level lasers with different spatial variations in the pumping rate. The parameters of our figures reflect those of fiber lasers. Both the uniform and Gaussian distributions are truncated at the laser medium radius R , which corresponds to the radius of the fiber core. The Gaussian waist W is assumed to equal this radius, $W=R$; see the inset to Fig. 2(a). We choose the cross-sectional area of the uniform mode to be that of the fiber core $A=\pi R^2$.

Since we are considering an incoherently pumped laser it may appear inconsistent to use a sinusoidal longitudinal mode associated with resonating the pump in a Fabry-Pérot cavity. However, the incoherently pumped three-level laser is the limit of a coherently pumped four-level laser with sufficiently rapid decay out of the upper pump level. The combined coherently pumped transition and spontaneous decay is then well approximated by a single incoherently pumped transition.

Figures 2(a) and 2(b) are plots of the (almost) zero-frequency squeezing spectral density calculated using Eq. (16) of the linearized P -function theory. In the spatially uniform case the best squeezing $V=0.5$ occurs when the pumping rate is matched to the spontaneous emission rate $P=0.5\gamma$. An interesting feature of the figures is that a spatially nonuniform pumping rate can increase the squeezing for a fixed integrated pumping rate P_I . However the maximum squeezing irrespective of pump rate is not increased. Note that the dimensionless integrated pumping rate parametrizing the figures, $P_I/(\gamma\pi R^2)$, is normalized by the spontaneous emission rate γ and by the laser medium cross-sectional area πR^2 .

Enhanced squeezing is possible with nonuniform spatial pumping because of the associated spread in rates about the uniform pumping rate $P_I/(\pi R^2)$. For a small but sufficiently large pumping rate there is some region of matching. At low pumping rates matching occurs to-

wards the mode peaks, while for high pumping rates it occurs towards the troughs. The peak pumping rate with Gaussian variation is twice that of the uniform case, and sinusoidal longitudinal variation increases it by a further factor of 2.

Low pumping rates are likely to be of most practical interest; see Fig. 2(b). In this region transverse variations alone do not significantly increase the squeezing, while the addition of sinusoidal longitudinal variation does. For $P=0.1$ the squeezing for the transversely and longitudinally varying pump is $V=0.67$, while for a uniform pump $V=0.72$. Since the squeezing for the Gaussian transverse variation alone is $V=0.72$, and for the

sinusoidal longitudinal variation alone (not shown in figures) is $V=0.66$, the enhancement is a result of the longitudinal pump rate variation.

Figure 2(c) shows the laser cavity mode photon number as a function of pumping rate. The laser output power is decreased by nonuniform spatial pumping. This is because the regions of higher pumping rate do not contribute proportionately more photons, due to laser saturation. Hence the reduced light output from regions of low pumping is not balanced by increases from regions of high pumping.

The effect of nonuniform pumping rates may also be calculated using the statistical model of sec. III. When \bar{g}_0 is large enough for the model to be valid over most of the mode its predictions are essentially the same as those of the P -function theory. The advantage of the statistical model is its simplicity.

In the limit of infinitely small volume elements the sum in Eq. (23) for the overall Fano factor becomes an integral

$$f = \int_V f(\mathbf{r}) \frac{\bar{n}(\mathbf{r})}{\bar{n}} \rho d^3r. \quad (31)$$

$f(\mathbf{r})$ is the Fano factor at position \mathbf{r} given by Eq. (20) with P_j replaced by $P(\mathbf{r})$. $\bar{n}(\mathbf{r})/\bar{n}$ is the proportion of photons contributed by the volume element d^3r at \mathbf{r} . According to the statistical model, the mean number of photons produced by a single atom in time T is T/\bar{t} , where \bar{t} was determined in the second paragraph of Sec. III. \bar{n} is the total cavity photon number, the integral of contributions over all volume elements

$$\bar{n} = \int_V \bar{n}(\mathbf{r}) \rho d^3r = \rho \int_V \frac{T}{\bar{t}} d^3r = \rho T \int_V \frac{\gamma P(\mathbf{r})}{2P(\mathbf{r}) + \gamma} d^3r. \quad (32)$$

For a transverse Gaussian pump these integrals may be evaluated exactly. Using cylindrical polar coordinates and assuming the medium volume to be a cylinder of length L and radius R we have

$$\begin{aligned} \bar{n} &= \rho TL \int_0^R \frac{\gamma P' e^{-2(r/W)^2}}{2P' e^{-2(r/W)^2} + \gamma} 2\pi r dr \\ &= \frac{1}{2} \rho TV_N \gamma \ln \left[\frac{2P' + \gamma}{2P'K + \gamma} \right], \end{aligned} \quad (33)$$

$$P' = P_1 L / V_N, \quad K = e^{-2(R/W)^2}, \quad V_N = \frac{1}{2} \pi W^2 L,$$

where P' is the peak pumping rate. The remaining integral is, using Eq. (20) for the Fano factor,

$$\begin{aligned} I &= \int_0^R f(\mathbf{r}) \bar{n}(\mathbf{r}) \rho d^3r \\ &= \rho TL \int_0^R \frac{\gamma^2 + 4P'^2 e^{-4(r/W)^2}}{(\gamma + 2P' e^{-2(r/W)^2})^2} \\ &\quad \times \frac{\gamma P' e^{-2(r/W)^2}}{2P' e^{-2(r/W)^2} + \gamma} 2\pi r dr. \end{aligned} \quad (34)$$

This evaluates to

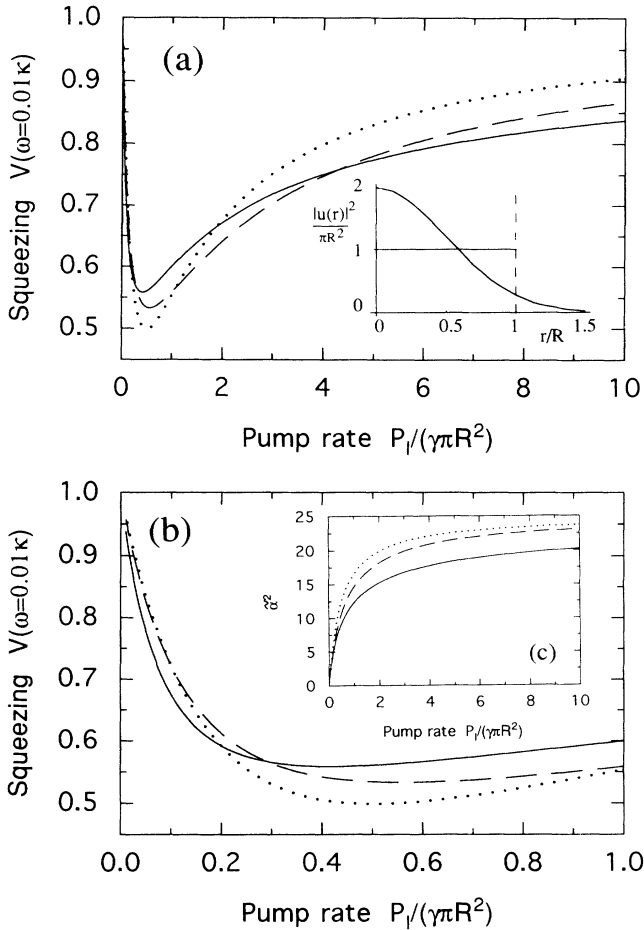


FIG. 2. Effect of spatially varying pump rates on the incoherently pumped three-level laser. The integrated pumping rate is expressed as the dimensionless quantity $P_1/(\gamma\pi R^2)$, where P_1 is defined by Eq. (25). The dotted line is the spatially uniform case, the dashed line the transverse Gaussian, and the solid line the combined transverse Gaussian and longitudinal standing wave. The Gaussian waist is equal to the radius of the mode, $W/R=1$. Other parameters are $\bar{g}/\gamma=1$ and $\kappa/\gamma=0.01$. (a) Plot of laser output amplitude squeezing $V(\omega=0.01\kappa)$ as a function of dimensionless pumping rate. Results obtained using Eq. (16). Inset shows the Gaussian and uniform mode functions considered. The vertical dashed line indicates the fiber core radius. (b) Zoom in on (a) for low pumping rates. Inset (c): Intracavity laser photon number per atom, $\bar{\alpha}$, as a function of pump rate. Obtained using Eq. (7).

$$I = \frac{1}{2} \rho T V_N \gamma \left\{ \gamma \frac{4P' + \gamma}{(2P' + \gamma)^2} - \gamma \frac{4P'K + \gamma}{(2P'K + \gamma)^2} + \ln \left[\frac{2P' + \gamma}{2P'K + \gamma} \right] \right\}. \quad (35)$$

The overall Fano factor for the laser is then $f = I/\bar{n}$. Recalling that $f \approx V(\omega=0)$, this agrees very well with the curves shown in Fig. 2.

3. The pumping rate: four-level laser

In this section the statistical model is used to determine the effect of spatial variations in the pumping rate on the coherently pumped four-level laser discussed in Ref. [5], and shown schematically in Fig. 3. This laser has a maximum squeezing of $V(\omega=0)=0.2$ at the pumping intensity $(E/\gamma)^2=0.13$.

Since the pump is coherent the time statistics of the overall pumping process must be determined using a master equation, as described in Ref. [5]. The parameter determining the pump rate is E . It is proportional to the pump field amplitude and to the Jaynes-Cummings coupling strength for the pump transition. It is defined fully by Eq. (2) of Ref. [5]. Solving the master equation describing the atomic transition from the lower lasing level $|2\rangle$ to the upper lasing level $|3\rangle$ via levels $|1\rangle$ and $|4\rangle$ gives the following time dependence of the population in level $|3\rangle$ [5]:

$$\sigma_3 = 1 + e^{-\gamma t} + [32E^2 - \gamma^2(e^{\Omega t} + e^{-\Omega t})] \frac{e^{-\gamma t/2}}{4\Omega^2}, \quad (36)$$

where $\Omega = (\gamma^2 - 16E^2)^{1/2}/2$, and the population is in state $|2\rangle$ at $t=0$. Ideal matching of the two incoherent decays has been assumed so that $0.5\gamma_{12} = \gamma_{34} = \gamma$. The mean time for the transition from level $|2\rangle$ to level $|3\rangle$ is, using Eq. (36),

$$\bar{t} = \int_0^\infty t \frac{d\sigma_3}{dt} dt = -\frac{1}{\gamma} - \frac{16E^2}{\Omega^2\gamma} - \frac{\gamma^2}{4\Omega^2} \frac{\gamma}{\Omega^2 - \gamma^2/4}, \quad (37)$$

and the mean-square time is

$$\bar{t}^2 = \int_0^\infty t^2 \frac{d\sigma_3}{dt} dt = -\frac{2}{\gamma^2} - \frac{64E^2}{\Omega^2\gamma^2} + \frac{\gamma^2}{\Omega^2} \frac{\Omega^2 + \gamma^2/4}{(\Omega^2 - \gamma^2/4)^2}. \quad (38)$$

The final quantity needed for the statistical model is the

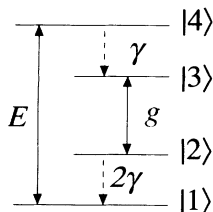


FIG. 3. Schematic diagram of the four-level coherently pumped laser's level scheme.

mean photon number produced per atom in time T ,

$$\bar{n}(r) = \frac{T}{\bar{t}} = T \frac{E^2}{(3E^2/\gamma + \gamma/4)}. \quad (39)$$

Using these formulas in Eq. (19), (21), and (23) gives the results shown in Fig. 4. As for the three-level case the maximum squeezing is reduced by the spatial variations of the pump. However, for a fixed pumping rate (pump power) spatial structure may increase the squeezing over that predicted for the uniform pump. As before, the advantage at low power comes from the sinusoidal longitudinal variation, rather than the Gaussian transverse variation.

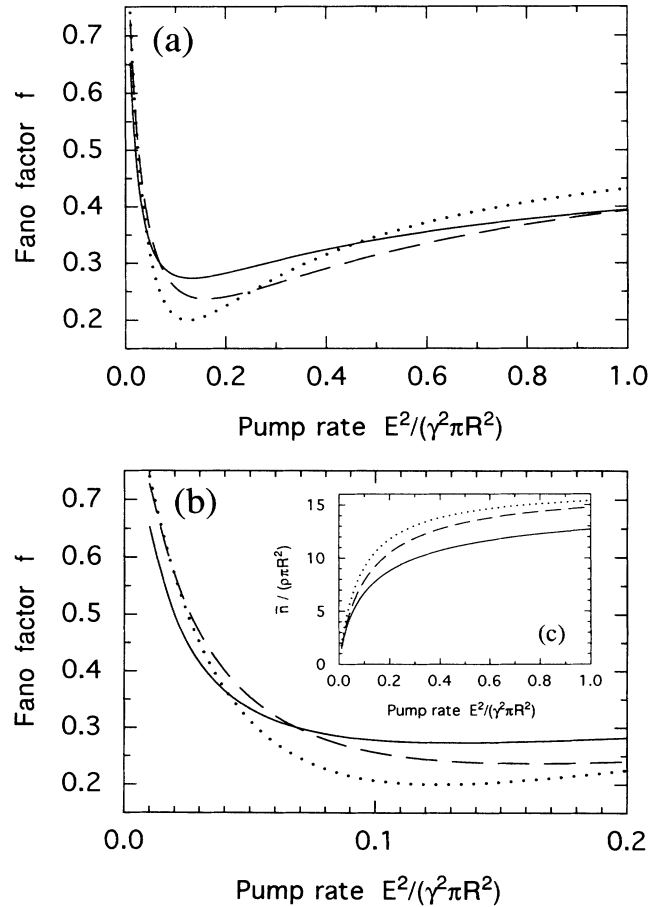


FIG. 4. Effect of spatially varying pumping intensity on the coherently pumped four-level laser. The pumping field is expressed as the dimensionless quantity $E/(\gamma^2\pi R^2)$. The dotted line is the spatially uniform case, the dashed line the transverse Gaussian, and the solid line the combined transverse Gaussian and longitudinal standing wave. Parameters are $W/R=1$, $\bar{g}/\gamma=1$, and $\kappa/\gamma=0.01$. (a) Plot of laser output Fano factor f as a function of dimensionless intensity of the coherent pump. Results obtained using Eq. (23). (b) Zoom in on (a) for low pumping rates. Inset (c): Intracavity laser photon number per atom, $\bar{n}/(\rho\pi R^2)$, as a function of pumping rate. Obtained using Eq. (39) with $T=1/2\kappa$, by integrating over the mode.

V. SUMMARY

We have included spatial structure in the calculation of laser squeezing. Since the statistical model of Sec. III is both simple and accurate a wide variety of lasers can be easily and accurately modeled. This offers the hope of obtaining excellent agreement between theory and experiment.

The preceding analyses showed that the spatial structure of the laser mode can be ignored in practice. This is because the coupling between the laser atoms and laser mode can easily be made much stronger than the minimum required for laser operation.

However, spatially nonuniform pumping can significantly increase or decrease the squeezing compared with the ideal spatially uniform case. The maximum squeezing as a function of pumping rate is always decreased. But in practice it may be difficult to achieve the high pumping rates corresponding to maximum squeezing and so the behavior at low pumping rates is of particular interest.

We have presented graphical results appropriate for a

fiber laser. Specifically we have used a Gaussian transverse profile which is truncated on the wings at a radius equal to the Gaussian waist. At this point the pumping rate is $1/e^2=0.14$ of the peak rate at the center. At low pumping rates nonuniform pumping only significantly affects the squeezing when there is both transverse and sinusoidal longitudinal variation. The squeezing is then increased, for a fixed total pump power. This would occur if the pump were optical and resonantly enhanced in a Fabry-Pérot cavity. Consequently, better squeezing is obtained if the pump cavity is a Fabry-Pérot cavity rather than a ring cavity. This result is potentially useful since the high pumping rates necessary for matching may require resonant enhancement.

In summary we have found that spatial structure can be accounted for and generally has a small impact on laser squeezing.

ACKNOWLEDGMENTS

We acknowledge discussions with A. Stevenson. This work is supported by the Australian Research Council.

-
- [1] A. M. Khazanov, G. A. Koganov, and E. P. Gordov, *Phys. Rev. A* **42**, 3065 (1990).
 - [2] T. C. Ralph and C. M. Savage, *Opt. Lett.* **16**, 1113 (1991).
 - [3] H. Ritsch, P. Zoller, C. W. Gardiner, and D. F. Walls, *Phys. Rev. A* **44**, 3361 (1991).
 - [4] H. Ritsch and P. Zoller, *Phys. Rev. A* **45**, 1881 (1992).
 - [5] T. C. Ralph and C. M. Savage, *Phys. Rev. A* **44**, 7809 (1991).
 - [6] D. L. Hart and T. A. B. Kennedy, *Phys. Rev. A* **44**, 4572 (1991).
 - [7] T. C. Ralph and C. M. Savage, *J. Opt. Soc. Am B* (to be published).
 - [8] Min Xiao, H. J. Kimble, and H. J. Carmichael, *Phys. Rev. A* **35**, 3832 (1987).
 - [9] D. M. Hope, D. E. McClelland, and C. M. Savage, *Phys. Rev. A* **41**, 5074 (1990).
 - [10] H. Haken, in *Laser Theory*, edited by S. Flugge, *Encyclopedia of Physics Vol. XXX/2c* (Springer-Verlag, Heidelberg, 1970).
 - [11] W. H. Louisell, *Quantum Statistical Properties of Radiation* (Wiley-Interscience New York, 1973).
 - [12] C. W. Gardiner, *Quantum Noise* (Springer-Verlag, Berlin, 1991).
 - [13] P. D. Drummond and C. W. Gardiner, *J. Phys. A* **13**, 2353 (1980).
 - [14] C. W. Gardiner, *Handbook of Stochastic Methods* (Springer-Verlag, Berlin, 1985).
 - [15] M. D. Reid, *Phys. Rev. A* **37**, 4792 (1988).
 - [16] C. W. Gardiner and M. J. Collett, *Phys. Rev. A* **31**, 3761 (1985).
 - [17] G. L. Squires, *Practical Physics*, 3rd ed. (Cambridge University Press, Cambridge, England, 1985).